Experimental Investigation of Impinging Shock – Cavity Interactions with Upstream Transverse Jet Injection

By Hossein ZARE-BEHTASH,[1)2)] Kin Hing LO,[1)] Takahiro UKAI,[2)] Konstantinos KONTIS[1)] and Shigeru OBAYASHI[2)]

[1)]*The University of Manchester, School of Mechanical Aerospace and Civil Engineering, Manchester, UK*
[2)]*University of Glasgow, School of Engineering, Glasgow G12 8QQ, UK*
[3)]*Institute of Fluid Science, Tohoku University, Sendai, Japan*

Mixing between the injected fuel and high speed free stream air is challenging at supersonic speeds. Placing cavities downstream of injection holes or slots addresses the problem of flame holding and stabilisation, however there are still open questions related to mixing enhancement, uniformity and efficiency. The present study examines experimentally the flow field interactions due to a transverse jet - cavity combination with shock impingement at supersonic speeds using PIV, Schlieren photography, and oil flow surface visualisation. The oblique shock lifts the shear layer over the cavity and combined with the instabilities generated by the transverse jet injection creates a highly complicated flowfield with numerous vortical structures. The interaction between the oblique shock and the jet leads to a relatively uniform velocity distribution within the cavity. The lifting of the shear layer is also believed to reduce the drag created by the cavity.

Key Words: Shock-Jet Interaction, Shock-Cavity Interaction, Jet-Cavity Interaction, Transverse Jet

1. Introduction

Jet injection into supersonic cross flows has applications in flow control, creation of forces and moments for attitude control, and most importantly in scramjets for supersonic combustion to take place [1-9]. Mai *et al.* [10] showed that by having an incident shock impinge downstream of a transverse jet injection location, enhanced mixing of the fuel and air can be achieved leading to increased residence time and more efficient combustion. Employing cavities is another mechanism to improve combustion in scramjets by decelerating the breathing air from supersonic to subsonic speeds for combustion to occur. Using a cavity for a flame holding mechanism Baurle *et al.* [11] injected fuel upstream and examined the combustion process experimentally and numerically. They found little entrainment of the injected fuel within the cavity. Sakamoto et al. [12] showed that using an impinging shock wave over the surface of an open cavity, the structures that occur within it can be controlled to enhance the mixing and also the flow stability within the cavity, with the location of the impingement playing a significant role.

It is the objective of the current investigation to analyse the fundamental flow physics when combining an impinging shock wave over a cavity with an upstream transverse jet injection. The impinging shock will be made to interact with the transverse jet and cavity at different locations. Using a rectangular open cavity, length/depth < 10, such as the one employed in this study, has been shown by Gruber *et al.* [13] to have relatively lower drag, however, at the same time the flow is unstable compared with cavities which have inclined aft walls.

It is believed that combing the merits of an impinging shock wave over a cavity with the benefits obtained when having a shock wave impinge downstream of a transverse jet, high levels of mixing and flow stability can be achieved. The impinging shock over the cavity, will lift the shear layer and therefore reduce the effect of the interaction with the aft wall which was reported by Sakamoto *et al.* [12].

2. Experimental Setup

2.1 Trisonic Wind Tunnel

The Aero-Physics Laboratory trisonic wind tunnel is an intermittent indraft wind tunnel. The general arrangement of the wind tunnel is shown in Fig. 1. The vacuum tank pressure is lowered to 25mbar before the butterfly valve is opened and the air is drawn from the ambient. The throat height at the supersonic inserts' location is approximately 100mm. The desiccant particles at the inlet absorb the moisture in the air to avoid liquefaction of the flow through the test section. The heater acts only to dry the desiccants and relieve them of any moisture content.

The wind tunnel testing area is split into three sections: 1) the supersonic inserts, 2) the test section, and 3) the diffuser section. Section 2, which is where the model and shock generator are placed, is a uniform area section with the dimensions of 150×215×485mm (width×height×length). The supersonic inserts were designed for a flow Mach number of 1.9. This was confirmed through pitot measurements at the centre of the test section, before the shock generator and cavity model were placed inside the wind tunnel. If the presence of the models had a significant impact on the freestream Mach number, the tunnel would unstart and we

would not achieve stable shocks originating from the shock generator and the cavity model.

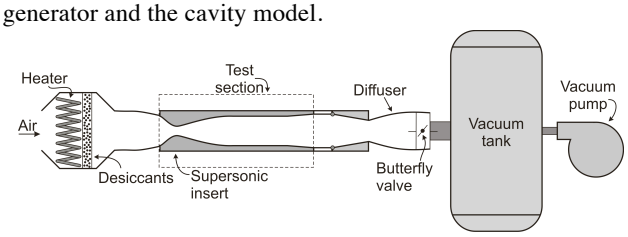

Fig. 1. Trisonic wind tunnel.

The tunnel has a stable run time of approximately 5 seconds for a Mach number of 1.9. For the same initial conditions the tunnel exhibits a Mach number variation of ±0.01 for different runs.

2.2. Model Geometry

A steel shock generator with a wedge angle of 10 degrees is used to generate an oblique shock wave which impinges over the cavity. This was mounted from the top wall of the test section.

A rectangular cavity, 100mm in length (L) and 20mm deep (D), was designed and manufactured, see . Based on the length and depth of the cavity, it is classified as an open cavity. An axisymmetric conical jet hole with an orifice diameter of d_i=2.2mm was placed 0.1L (10mm) upstream of the cavity. High pressure air was supplied through a regulator into the jet hole. The jet pressure was adjusted to provide a jet to freestream momentum flux ratio of 5.3, which is defined in Eq. (1),

$$J = \frac{\gamma_{jet}\rho_{jet}M_{jet}^2}{\gamma_o\rho_o M_o^2} \quad (1)$$

where γ is the specific heat ratio, ρ is the density, M is the Mach number and subscripts "o" and "jet" refer to the freestream and jet conditions, respectively [14]. The momentum flux ratio is a measure of the jet penetration into the freestream. The Mach number of the jet was determined by measuring the total pressure of the jet before discharge and the jet static pressure during discharge. The jet density was determined from standard tables based on the Mach number.

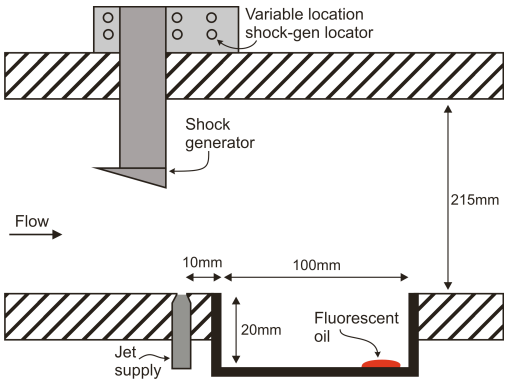

Fig. 2. Test section geometry.

2.3. Fluorescent Oil Flow

The oil flow recipe used in the current setup has been optimised for the current experimental conditions. This ensures that the oil does not dry too quickly, allowing sufficient time for the flow to establish, but at the same time it is not so viscous that it does not follow the flow streamlines.

The formulation uses fluorescent powder suspended in paraffin, oleic acid, and silica gel. Before each run, the oil is deposited inside the cavity near the rear wall, as shown in Figure 2, and illuminated with UV LED panels from both sides of the test section. Images were acquired using a Canon SLR camera, model EOS-450D, with 12M pixel resolution.

2.4. Schlieren Photography

High-speed schlieren photography [15, 16] was employed to visualise the flow. A 450W continuous Xenon lamp is used as the illumination source. The light passes through a plano-convex lens with 75 mm diameter and 75 mm focal length. The converged light spot passes through an iris with a variable aperture of 3–50 mm and is finally cut by a slit. The resulting light beam is collimated using a parabolic mirror of 203.3 mm diameter and 1016 mm focal length. The collimated light passes through the test region and is then de-collimated by another parabolic mirror. The focal point of the second mirror is on a knife edge. The amount of light cut-off could be controlled by the knife edge which affected the sensitivity of the system. The experiments were carried out in dark conditions. A Photron SA-1 high-speed camera was used to capture images at a frame rate of 10kfps with an exposure time of 1μs. The setup is presented in Fig. 3 and has been successfully used in the past [17].

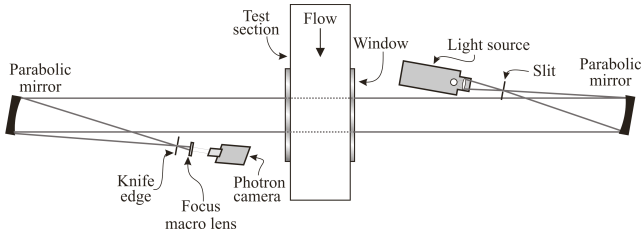

Fig. 3. Z-type schlieren photography setup.

2.5. Particle Image Velocimety

A Litron Nano L series, ND:YAG Q-switched laser is used for particle image velocimetry (PIV) illumination. The laser has a pulse energy of 200mJ with a repetition rate of 15Hz. The laser beams are pulsed at a wavelength of 532 nm with a pulse duration of 4ns. Time averaged flow field measurements consisting of 40 pairs of images with a Δt of 0.9μs, so that sufficient displacement of the tracer particles suitable for the present velocity range could be achieved. A laser arm was used to deliver the laser to the test section. The laser sheet is placed perpendicular to the camera.

A TSI six-jet atomiser TSI model 9307-6 was used to create seeder particle with particle diameters of approximately 1μm [18]. A LaVision Imager ProX2M CCD camera with

1600×1200 pixel resolution captured the scattered light from the particles. The camera records images at 14 bit digitisation. The recorded image pairs are initially divided into 32×32 pixel interrogation windows and then processed with a cross correlation algorithm using the DaVis 7.2 software. The interrogation windows are then refined to 16×16 pixel squares. A 50% overlap is employed in order to improve spatial resolution and to prevent the appearance of spurious vectors by adaptively moving the interrogation window [19].

3. Results and Discussions

The instantaneous schlieren photographs corresponding to the jet off and on cases are presented in Fig. 4. As evident from the figures, the interaction between the oblique incident shock creates a flow feature similar to an SBLI, namely the lifting of the shear layer. This behavior is also encountered when a shock impinges on a boundary layer over a flat surface. The interaction of a transverse jet in a cross flow leads to the creation of large scale vortex structures along the boundary of the jet as well as small vortices which appear before and aft of the jet injection location [20, 21]. A bow shock also appears and stands upstream from the jet injection location due to the obstruction induced by the transverse jet.

From the schlieren images, it appears that the shear layer over the cavity is more turbulent when the jet is switched on. A shock wave appears at the aft wall of the cavity indicating the presence of supersonic flow.

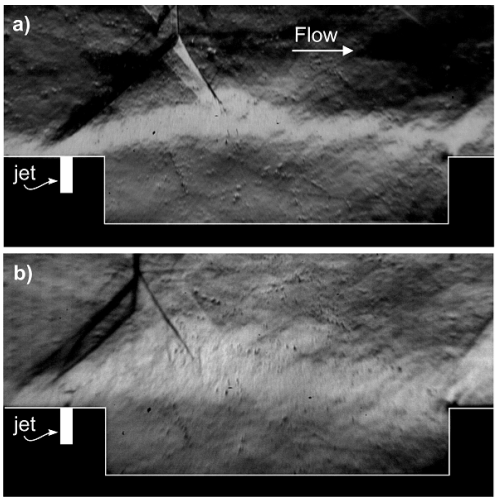

Fig. 4. Schlieren photographs of the flow with (a) jet off, (b) jet on.

Figure 5 shows time averaged schlieren images corresponding to the jet off and jet on cases. These were obtained by taking the average of 200 instantaneous images. When the jet is switched on, the between the jet and the incoming flow creates large-scale vortex structures leading to the turbulisation of the boundary layer. When the incident shock impinges on this separated boundary layer, which now forms the shear layer, it further amplifies these vortex structures creating a more turbulent and thicker boundary layer. Comparing Figures 5(a) and 5(b), the shear layer is clearer in Figure 5(a), this suggests that in the individual instantaneous schlieren images the shear layer has the same thickness and properties so that when these images are superimposed and averaged they all tend to give the same flow property. However, if the flow were to be very turbulent, then each schlieren image would depict the boundary layer slightly different than the other images.

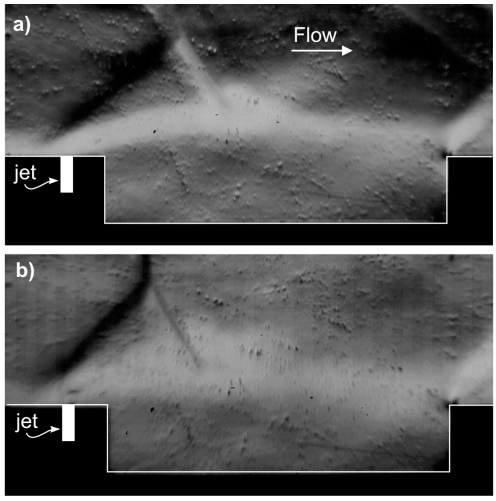

Fig. 5. Time-averaged schlieren photographs of the flow with (a) jet off, (b) jet on.

The oil flow pattern on the cavity floor presented in Fig. 6, along with a schematic showing the area which the oil flow images relate to inside the cavity, it is evident that the separation line of the main vortex, corresponding to the recirculation zone within the cavity, moves up when the jet is switched on. This indicates a larger recirculation region inside the cavity

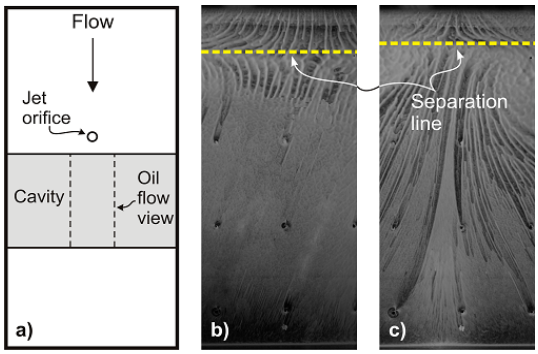

Fig. 6. Oil flow along the cavity floor (a) schematic of field of view, (b) jet off, (c) jet on.

The velocity field, with the flow from left to right, presented in Fig. 7(a) displays clearly the shock structures visible in the schlieren images of Fig. 4. Because the laser sheet was shined from the top of the test section at an angle, there is a small portion inside the cavity near the rear aft wall which did not receive any laser light and is therefore masked

out from the processing. From the interaction point of the oblique shock and the bow shock from the jet, a slipstream emerges which is also captured. The velocity contours show the lifting of the shear layer by the oblique shock, the drop in it afterwards, and the shock which forms at the apex of the rear wall of the cavity. When the jet is switched on, Fig. 7(b), the flowfield changes dramatically.

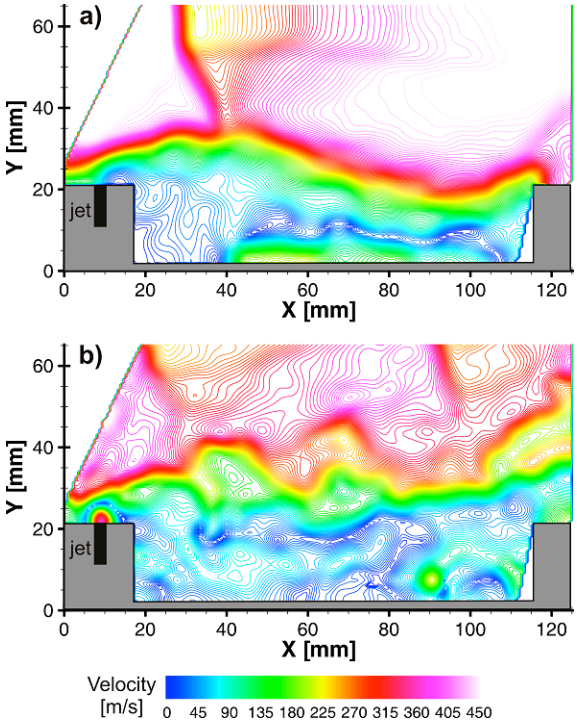

Fig. 7. Absolute velocity field of (a) jet off, (b) jet on.

The boundary of the shear layer becomes very distorted as a result of the amplification of the vorticies induced by the transverse jet. Another difference between the two cases, with and without the transverse jet, is the velocity distribution inside the cavity. When the jet is switched on, the non-uniformity in velocity field due to the lifting of the shear layer by the impinging shock is less noticeable. This is because the shear layer after the impingement location is also raised. Because of this, the shock wave which is formed at the apex of the rear cavity wall is also weaker. This is a very significant outcome, since the presence of this shock leads to considerable drag within a supersonic combustor. Due to the high-speed transverse jet there is a lack of seeder particles in the immediate vicinity of the jet, therefore the velocity field in this location is not reliable.

Breaking down the velocity field of Fig 7 into only the x-component of velocity, Vx, shown in Fig. 8(a), one can see the area of flow reversal inside the cavity adjacent to the bottom wall. With the introduction of the jet in Fig. 8(b) the strength of this reversed flow region is greatly reduced. In the main flowfield outside the cavity, the introduction of the jet and the formation of the oblique shock ahead of the jet causes a compression of the freestream and the reduction in streamwise velocity.

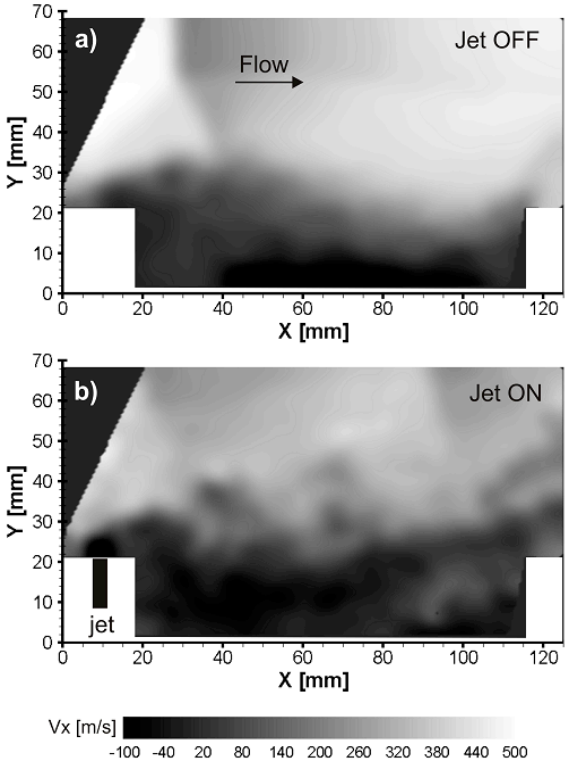

Fig. 8. Instantaneous Vx (a) jet off, (b) jet on case.

Analysis of the Vy component of velocity in Fig. 9 reveals an interesting flow feature. Immediately after the impingement location of the incident shock a strong downward velocity component exists. This region is due to the presence of an expansion wave that deflects the flow towards the cavity after it has been lifted by the incident shock.

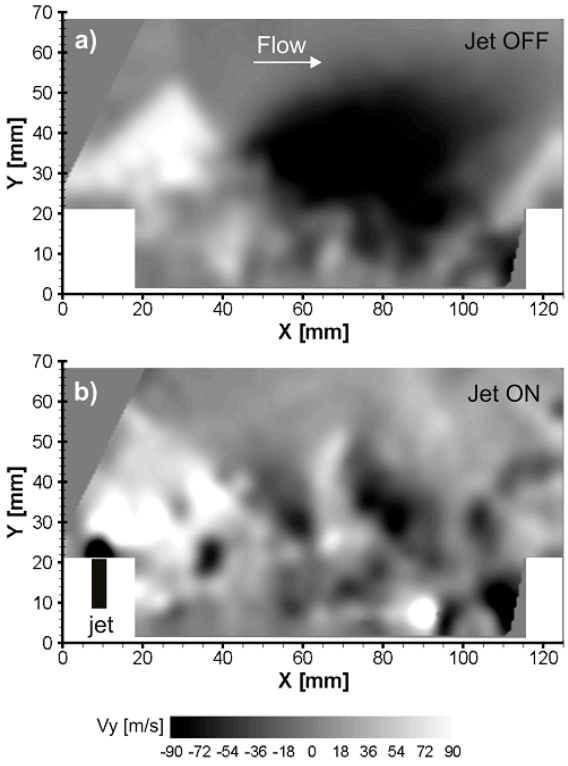

Fig. 9. Instantaneous Vy (a) jet off, (b) jet on case.

Based on the PIV data, the vorticity of the flow is calculated and presented in Fig. 10, the flow is from left to right. In Fig. 10(a) the slipstream from the shock interactions is clearly visible. The main vortex structures in this figure originate from the separation shock created upstream of the cavity.

The interaction of the shear layer and the oblique shock leads to the creation of vortex structures inside the cavity, the majority of which are located towards the aft wall inside the cavity. The combination of the injected transverse jet flow and the oblique shock influence creates numerous vortical structures inside the cavity, see Fig. 10(b), which in contrast to Fig. 10(a) are distributed throughout the entire cavity area and not just near the aft wall.

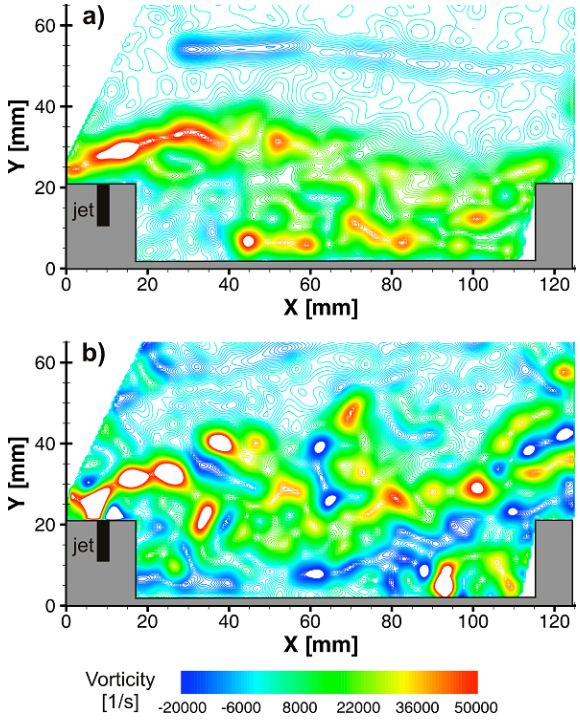

Fig. 10. Vorticity field corresponding to (a) no jet, (b) jet.

7. Conclusions

The current study examined the effect of an oblique shock impinging over a shear layer on a cavity with an upstream transverse jet injection. Understanding jet-cavity interactions are vital for achieving efficient supersonic combustion through stable flameholding and good mixing between the injected fuel and the air.

Valuable PIV data obtained demonstrates that the combination of the oblique shock and the upstream transverse jet leads to the lifting of the shear layer and the hence reduction in the drag created on the aft cavity wall.

Further studies involving pressure sensitive paints are underway to further understand the flow physics and interactions involved. Different jet momentum flux ratios will also be investigated.

8. Future Work

High-speed PIV measurements will be conducted to obtain time average velocity and vorticity fields as well as rms properties of the velocities Vx and Vy.

The location of the impinging shock and that of the jet injection will be varied to examine their effect on mixing inside the cavity. The Reynold stress will be calculated for each case to provide a better understanding of the mixing that occurs inside the cavity.

Using infra-red tomography the heat transfer inside the cavity floor will be examined to provide more insight into the physical properties of the flowfield.

Acknowledgments

The authors are indebted to the technical and administrative staff of the School of MACE at Manchester University, especially Mr. Lee Paul for the manufacture of the models. The support of the EPSRC Engineering Instrument Pool for the loan of the Photron high-speed camera is also greatly acknowledged.

References

1) Cecere, D., Ingenito, A., Giacomazzi, E., Romagnosi, L., and Bruno, C.: Hydrogen/air supersonic combustion for future hypersonic vehicles, *International Journal of Hydrogen Energy* **36** (2011), pp. 11969-11984.
2) Erdem, E., and Kontis, K.: Numerical and experimental investigation of transverse injection flows, *Shock Waves* **20** (2010), pp. 103-118.
3) Gruber, M.R., Nejad, A.S., Chen, T.H., and Dutton, J.C.: Transverse injection from circular and elliptic nozzles into a supersonic crossflow, *Journal of Propulsion and Power* **16**(3) (2000), pp. 449-457.
4) Ali, M., Fujiwara, T., and Leblanc, J.E.: Influence of main flow inlet configuration on mixing and flameholding in transverse injection into supersonic airstream, *International Journal of Engineering Science* **38** (2000), pp. 1161-1180.
5) Lee, S.H.: Characteristics of dual transverse injection in scramjet combustor, Part 1: Mixing, *Journal of Propulsion and Power* **22**(5) (2006), pp. 1012-1019.
6) Lee, S.H.: Characteristics of dual transverse injection in scramjet combustor, Part 2: Combustion, *Journal of Propulsion and Power* **22**(5) (2006), pp. 1020-1026.
7) Tomioka, S., Jacobsen, L.S., and Schetz, J.A.: Sonic injection from diamond-shaped orifices into a supersonic crossflow, *Journal of Propulsion and Power* **19**(1) (2003), pp. 104-114.
8) Ben-Yakar, A., and Hanson, R.K.: Cavity flame-holders for ignition and flame stabilization in scramjets: An overview, *Journal of Propulsion and Power* **17**(4) (2001), pp. 869-877.
9) Burtschell, Y., and Zeitoun, D.E.: Numerical investigation of H2 injection in Mach 5 air flow with a strong shock/boundary layer interaction, *Shock Waves* **13** (2004), pp. 465-472.
10) Mai, T., Sakimitsu, Y., Nakamura, H., Ogami, Y., Kudo, T., and Kobayashi, H.: Effect of the incident shock wave interacting with

transversal jet flow on the mixing and combustion, *Proceedings of the Combustion Institute* **33** (2011), pp. 2335-2342.

11) Baurle, R.A., Mathur, T., Gruber, M.R., and Jackson, K.R.: A numerical and experimental investigation of a scramjet combustor for hypersonic missile applications (1998), AIAA 98-3131.
12) Sakamoto, K., Matsunaga, K., Fujii, K., and Tamura, Y.: Experimental investigation if supersonic internal cavity flows (1995), *26th AIAA Fluid Dynamics Conference*, San Diego, AIAA 95-2213.
13) Gruber, M.R., Baurle, R.A., Mathur, T., and Hsu, K.-Y.: Fundamental studies of cavity-based flameholder concepts for supersonic combustors, *Journal of Propulsion and Power* **17**(1) (2001), pp. 146-153.
14) Huang, W., Liu, W.D., Li, S.B., Xia, Z.X., Liu, J., and Wang, Z.G.: Influences of the turbulence model and the slot width on the transvere slot injection flow field in supersonic flows, *Acta Astronautica* **73** (2012), pp. 1-9.
15) Settles, G.S.: Schlieren and Shadowgraph Techniques, *Springer* (2001).
16) Oh, J.-S., Olabanji, O.T., Hale, C., Mariani, R., Kontis, K., and Bradley, J.W.: Imaging gas and plasma interactions in the surface-chemical modification of polymers using micro-plasma jets, *Journal of Applied Physics* **44** (2011), pp. 1-6.
17) Zare-Behtash, H., Gongora-Orozco, N., Kontis, K., and Holder, S.J.: Application of novel pressure-sensitive paint formulations for the surface flow mapping of high-speed jets, *Experimental Thermal and Fluid Sciences* **33** (2009), pp. 852-864.
18) Zare-Behtash, H., Kontis, K., Gongora-Orozco, N., and Takayama, K.: Shock wave-induced vortex loops emanating from nozzles with singular corners, *Experiments in Fluids* **49** (2010), pp. 1005-1019.
19) Erdem, E., Saravanan, S., Lin, J., and Kontis, K.: Experimental investigation of transverse injection flowfield at Mach 5 and the influence of impinging shock wave (2012), *18th AIAA/3AF International Space Planes and Hypersonic Systems and Technologies Conference*, AIAA-2012-5800.
20) Aswin, G., and Chakraborty, D.: Numerical simulation of transverse side jet interaction with supersonic free stream, *Aerospace Science and Technology* **14** (2010), pp. 295-301.
21) Kawai, S., and Lele, S.K.: Large-eddy simulation of jet mixing in supersonic crossflows, *AIAA Journal* **48**(9) (2010), pp. 2063-2083.